Solid State Sciences 12 (2010) 1567–1569

Contents lists available at ScienceDirect

Solid State Sciences

journal homepage: www.elsevier.com/locate/ssscie

MgZnO/ZnO *p*–*n* junction UV photodetector fabricated on sapphire substrate by plasma-assisted molecular beam epitaxy

W.W. Liu [a,b], B. Yao [a,*], B.H. Li [a], Y.F. Li [a,b], J. Zheng [a,b], Z.Z. Zhang [a], C.X. Shan [a], J.Y. Zhang [a], D.Z. Shen [a], X.W. Fan [a]

[a] Key Laboratory of Excited State Processes, Chinese Academy of Sciences, Changchun 130033, China
[b] Graduate School of the Chinese Academy of Science, Beijing 100049, China

ARTICLE INFO

Article history:
Received 1 June 2010
Received in revised form
26 June 2010
Accepted 29 June 2010
Available online 21 July 2010

Keywords:
Photodetector
p–*n* Junction
MgZnO
Film

ABSTRACT

We have investigated the spectral response of back- and front-surface-illumination MgZnO/ZnO *p*–*n* ultraviolet photodetector fabricated by plasma-assisted molecular beam epitaxy on sapphire substrate. The current–voltage measurements show that the device has a rectifying behavior with a turn-on voltage of 4.5 V. The detector exhibits a broad spectral response which covers the visible and UV spectra regions (from 275 to 375 nm) and has a maximum peak response at the wavelength of 330 nm. At a reverse bias of 5 V, the visible rejection (R330 nm/R500 nm) was more than two orders of magnitude. The peak responsivity at 330 nm for the device under back-illumination is about four times larger than that of the device under front-illumination under the same reverse bias. The response mechanisms of the device under back- and front-illumination are discussed.

1. Introduction

Ultraviolet (UV) photodetection has drawn great deal of interest in resent years, due to its potential applications in such areas as solar astronomy, missile plume detection, space-to-space transmission, fire alarms and combustion monitoring [1–6]. For these applications, a photodetector should be able to sensitively respond in visible and UV spectra regions. Among many semiconductors, alloys of MgZnO are becoming the semiconductor of choice for ultraviolet (UV) photodetectors and light emitters. Due to their thermal stability and radiation hardness, these materials are remarkable tolerant in aggressive environments [7,8]. Furthermore, it has unique figures of merit such as availability of lattice-matched single-crystal substrates, relatively low growth temperatures and intrinsic visible blindness, which are crucial for practical optoelectronic devices [9–13]. By designing different Mg mole fraction, the cutoff wavelength of MgZnO based detectors can be adjusted in a wide UV range from 380 to 160 nm [10]. This approach makes selective UV spectral detection realizable. Among various structures which were applied to produce MgZnO based photodetectors, *p*–*n* and *p*–*i*–*n* photodiodes are considered to be the most suitable choice for the advantages of fast responding speed, low dark current and working without applied bias [14]. However, only few reports on MgZnO *p*–*n* or *p*–*i*–*n* photodiodes for UV detection, which was attributed to that it has a difficulty in obtaining high quality and reliable *p*-type MgZnO layer [15–22].

In the present work, a UV photodetector based on a heterojunction of *p*-MgZnO/*n*-ZnO was fabricated. The response was charactered under back- and front-illumination patterns. A broad spectral response covers the visible and UV spectra regions was obtained under both back- and front-illumination patterns, but the responsivity under back-illumination is always higher than that of the device under front-illumination. The response mechanisms of the device under back- and front-illumination were investigated.

2. Experimental section

The schematic diagram of the MgZnO/ZnO *p*–*n* junction UV photodetector structure is shown in Fig. 1. The semiconductor layers were deposited on a *c*-plane sapphire substrate by plasma-assisted molecular beam epitaxy (PA-MBE) growth technique. A *p*-MgZnO layer with a thickness of 600 nm and hole concentration of 2.89×10^{16} cm^{-3} was first deposited, followed by an *n*-ZnO layer with a thickness of 200 nm and electron concentration of 1.24×10^{18} cm^{-3}. For the growth of the *p*-MgZnO layer, 6 N-purity Zn, 6 N-purity Mg and 6 N-purity Li were used as the Zn, Mg and Li sources, respectively. 5 N-purity NO plasma was used as O source and N dopant. The details of the growth processes for the *p*-MgZnO

* Corresponding author. Tel.: +86 431 86176355; fax: +86 431 85682964.
E-mail address: yaobin196226@yahoo.com.cn (B. Yao).

1293-2558/$ – see front matter © 2010 Elsevier Masson SAS. All rights reserved.
doi:10.1016/j.solidstatesciences.2010.06.022

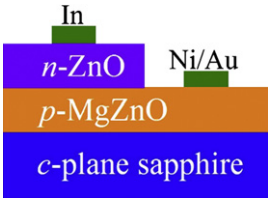

Fig. 1. The schematic diagram of the *p*–*n* junction UV photodetector structure.

layer will be reported elsewhere. The unintentionally doped ZnO layer was grown successively as *n*-type layer. Ni/Au and In electrodes were deposited by vacuum evaporation and used to form Ohmic contacts to the *p*-type and the *n*-type layer, respectively. The contacts were annealed in air atmosphere at temperature of 300 °C for 90 s.

The structure of the layers were characterized by a D/max-RA X-ray diffractometer (XRD) (Rigaku International Corp., Japan) with CuKα radiation ($\lambda = 0.1542$ nm), and all the diffraction peaks were calibrated by the (006) diffraction peak of the Al_2O_3 at 41.68°. Room temperature absorption and transmission spectrum were recorded using a UV–visible-near infrared spectrophotometer (Shimadzu). The spectral response of the detector was measured using a 150 W Xe lamp, monochromator, chopper (EG&G 192), and lock-in amplifier (EG&G 124A). The dark current was measured by a Hall analyzer (Lakeshore7707) with a sensitivity of 0.1 pA at room temperature.

3. Results and discussion

X-ray diffraction (XRD) patterns of the *p*-MgZnO and *n*-ZnO films were shown in Fig. 2, respectively. Besides (006) diffraction peak of the sapphire substrate, only a sharp diffraction peak corresponding to ZnO (002) plane was observed, suggesting that both of the films have preferred *c*-axis orientation. Full width at half maximum (FWHM) of the (002) diffraction peak of the *p*-MgZnO and *n*-ZnO films is 0.21° and 0.14°, respectively, which implied that both of the films have better crystal quality. Comparing with *n*-ZnO film, *p*-MgZnO film has a larger FWHM, which was attributed to the degradation of the crystal quality for the incorporation of Mg and *p*-type dopant.

Fig. 3 shows the absorption and transmission spectrum of the *p*-MgZnO/*n*-ZnO heterojunction grown on sapphire substrate. The absorption spectra shows two sharp absorption edges located at 340 nm and 375 nm. According to the relationship between the band gap and Mg content in the layers, these two absorption edges correspond to the band edge of the *p*-MgZnO and *n*-ZnO layers, respectively [10]. From transmission spectra, it is clearly seen that

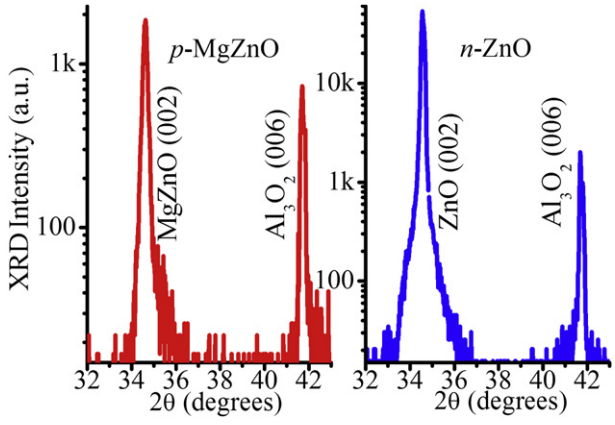

Fig. 2. XRD patterns of the *p*-MgZnO and *n*-ZnO layers.

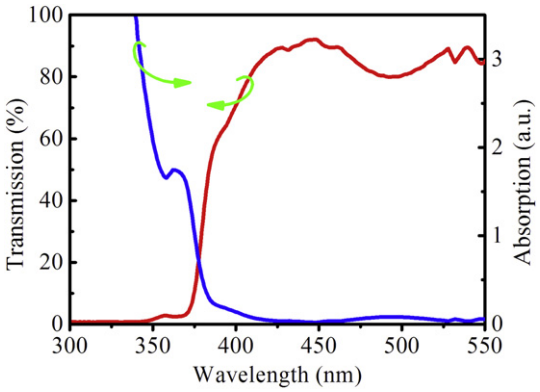

Fig. 3. Spectrum of the optical absorption and transmission of the *p*-MgZnO/*n*-ZnO heterojunction deposited on *c*-plane sapphire.

the sample has more than 80% transmission in the visible region. Two sharp absorption edges and high transmissivity implied that *p*-MgZnO/*n*-ZnO heterojunction with high quality was successfully fabricated on sapphire substrate.

I–*V* characteristic of the detector in semi-logarithmic drawing was shown in Fig. 4. Weak rectifying behavior for the device is observed. The bottom left and bottom right insets in Fig. 4 show the linear *I*–*V* curves of *n*–*n* contact on ZnO layer and *p*–*p* contact on MgZnO layer, respectively, indicating the formation of Ohmic contacts. The Ohmic behavior of metal contacts on top of ZnO and MgZnO layers excludes the possibility of formation any Schottky junctions in the device. This result indicates that the rectifying behavior comes from the *p*–*n* junction instead of the metal–semiconductor contacts. The turn-on voltage is about 4.5 V under forward bias and relatively low leakage current of 30 nA at a reverse bias of 5 V is observed. The deviation from that of the ideal *p*–*n* junction suggests that there might be several current transportation mechanisms in the junction due to the poor electrical properties of the *p*-MgZnO film at room temperature. The weak rectifying behavior also confirmed the poor quality of the *p*–*n* junction.

Fig. 5 shows the spectral response of the detector under back- and front-illumination at reverse bias of 5 V. The schematic diagrams of the back- and front-illumination patterns were shown in Fig. 6. The peak responsivity at 330 nm for the device under back- and front-illumination is about 2.16 mA/W and 0.53 mA/W, respectively, which was larger than the value reported previously

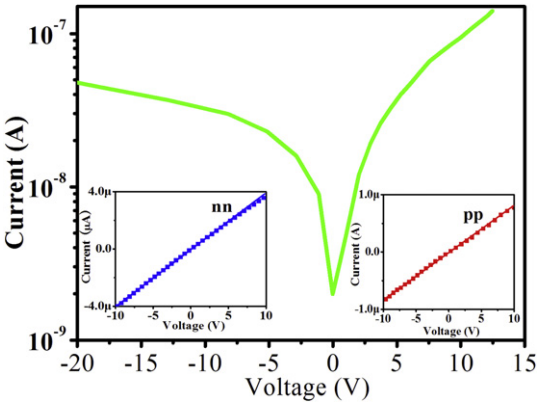

Fig. 4. Characteristic current–voltage (*I*–*V*) curve of the detector, the insert is *I*–*V* curve of Au/Ni metal contacts on *p*-MgZnO (red) and In metal contacts on *n*-ZnO (blue) (For interpretation of the references to colour in this figure legend, the reader is referred to the web version of this article).

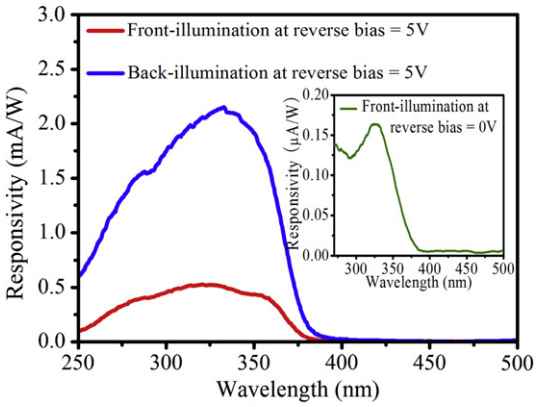

Fig. 5. The spectral response at reverse bias of 5 V for the detector under back- and front-illumination. The insert is the spectral response at zero-bias for the device under front-illumination.

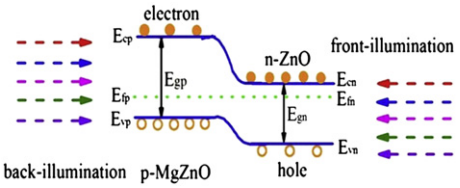

Fig. 6. The energy band diagram of the *p*-MgZnO/*n*-ZnO heterojunction (Front-illumination pattern denotes the device was illuminated on ZnO layer, while back-illumination pattern denotes the device was illuminated on MgZnO layer).

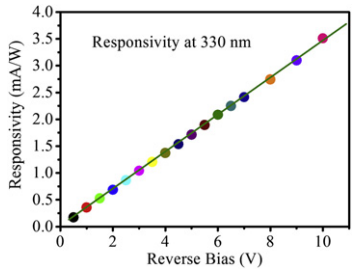

Fig. 7. The responsivity as a function of reverse bias voltage under front illuminated.

[19,20]. The spectral response at zero-bias for the detector under front-illumination was shown in the inset of the Fig. 5. It shows that the cutoff wavelength of the photodetector occurs at 340 nm which corresponds to the band gap of the *p*-MgZnO films and the UV/visible rejection ratio more than two orders of magnitude. These indicate that the device has high spectral selectivity. Fig. 7 is the responsivity as a function of reverse bias voltage under front-illumination. A linear relationship was obtained between 0.5 and 10 V, indicating no carrier mobility saturation or sweep-out effect up to 10 V reverse bias.

From Fig. 5, it can be found that the detector based on heterojunction of *p*-MgZnO/*n*-ZnO exhibits an enhancement in responsivity under back-illumination. The peak responsivity at 330 nm for the device under back-illumination is about four times larger than that of the device under front-illumination under the same reverse bias of 5 V. The device also exhibits higher responsivity in the 275–375 nm spectral regions. Under front-illumination at these wavelengths, as shown in Fig. 6, the optical penetration depth in *n*-ZnO decreases and surface recombination becomes a dominant factor in reducing the responsivity of the device. By employing back-illumination at these wavelengths, as also shown in Fig. 6, the penetration depth is increased in *p*-MgZnO layer and effects of surface recombination are minimized. In addition, the *p*-MgZnO layer also absorbs at these wavelengths and contributes to the increased responsivity.

4. Conclusions

p-type MgZnO based *p*–*n* heterojunction UV photodetector was fabricated on *c*-plane sapphire substrate. The device shows a rectifying behavior with a turn-on voltage of 4.5 V. The detector was able to sensitively respond in visible and UV spectra regions and has a largest peak response at the wavelength of 330 nm. The ultraviolet–visible rejection ratio of the detector was more than two orders of magnitude. Comparing with front-illumination, enhancement in peak responsivity at 330 nm under back-illumination was achieved for the reduction of the surface recombination velocity. With the improvement of the optical and electrical properties of the *p*-type MgZnO layer with different Mg content, we believed that the development of back-illumination MgZnO based *p*–*n* junction photodetector will pave the way for high-speed solar-blind detection applications.

Acknowledgments

This work is supported by the Key Project of the National Natural Science Foundation of China under Grant No 50532050; The Knowledge Innovation Program of the Chinese Academy of Sciences (NO. KJCX3.SYW.W01); The National Natural Science Foundation of China (Nos. 60776011, 60806002 and 10874178). The authors also would like to acknowledge financial support through Swedish Research Links via VR.

References

[1] M. Razeghi, A. Rogalski, J. Appl. Phys. 79 (1996) 7433.
[2] P. Schreiber, T. Dang, G. Smith, T. Pickenpaugh, P. Gehred, C. Litton, Proc. SPIE 230 (1999) 3629.
[3] T. Tut, T. Yelboga, E. Ulker, E. Ozbay, Appl. Phys. Lett. 92 (2008) 103502.
[4] M.Y. Liao, Y. Koide, J. Alvarez, Appl. Phys. Lett. 90 (2007) 123507.
[5] V.V. Kuryatkov, H. Temkin, J.C. Campbell, R.D. Dupuis, Appl. Phys. Lett. 78 (2001) 3340.
[6] R. Yousefi, F.J. Sheini, M.R. Muhamad, M.A. More, Solid State Sci. (2010). doi:10.1016/j.solidstatesciences.2010.04.019.
[7] D.C. Look, Mater. Sci. Eng. B 80 (2001) 383.
[8] F.D. Auret, S.A. Goodman, M. Hayes, M.J. Legodi, H.A. van Laarhoven, D.C. Look, Appl. Phys. Lett. 79 (2001) 3074.
[9] S. Choopun, R.D. Vispute, W. Yang, R.P. Sharma, T. Venkatesan, H. Shen, Appl. Phys. Lett. 80 (2002) 1529.
[10] A. Ohtomo, M. Kawasaki, T. Koida, K. Masubuchi, H. Koinuma, Y. Sakurai, Y. Yoshida, T. Yasuda, Y. Segawa, Appl. Phys. Lett. 72 (1998) 2466.
[11] Ming Song Wang, Eui Jung Kim, Eun Woo Shin, Jin Suk Chung, Sung Hong Hahn, Chinho Park, J. Phys. Chem. C 112 (2008) 1920.
[12] D.C. Look, D.C. Reynolds, J.W. Hemsky, R.L. Jones, J.R. Sizelove, Appl. Phys. Lett. 75 (1999) 811.
[13] T. Pauporté, E. Jouanno, F. Pellé, B. Viana, P. Aschehoug, J. Phys. Chem. C 113 (2009) 10422.
[14] S.M. Sze, Physics of Semiconductor Devices, second ed. Wiley, New York, 1981, pp. 582.
[15] J.L. Lyons, A. Janotti, C.G. Van de Walle, Appl. Phys. Lett. 95 (2009) 252105.
[16] S.B. Zhang, S.H. Wei, Alex Zunger, Phys. Rev. B 63 (2001) 075205.
[17] C. Klingshirn, Phys. Stat. Sol. B 244 (2007) 3027.
[18] B. Yao, D.Z. Shen, Z.Z. Zhang, X.H. Wang, Z.P. Wei, B.H. Li, Y.M. Lv, X.W. Fan, L.X. Guan, G.Z. Xing, C.X. Cong, Y.P. Xie, J. Appl. Phys. 99 (2006) 123510.
[19] K.W. Liu, D.Z. Shen, C.X. Shan, J.Y. Zhang, B. Yao, D.X. Zhao, Y.M. Lu, X.W. Fan, Appl. Phys. Lett. 91 (2007) 201106.
[20] Y.F. Li, B. Yao, R. Deng, B.H. Li, J.Y. Zhang, Y.M. Zhao, D.Y. Jiang, Z.Z. Zhang, C.X. Shan, D.Z. Shen, X.W. Fan, Y.M. Lu, J. Phys. D: Appl. Phys. 42 (2009) 105102.
[21] C.H. Park, S.B. Zhang, Su H. Wei, Phys. Rev. B 66 (2002) 073202.
[22] C.Y. Zhang, X.M. Li, J.M. Bian, W.D. Yu, X.D. Gao, Solid State Commun. 132 (2004) 75.